Published in final edited form as:

ChemMedChem. 2014 October ; 9(10): 2360–2373. doi:10.1002/cmdc.201402098.

Development of Diaminoquinazoline Histone Lysine Methyltransferase Inhibitors as Potent Blood-stage Anti-Malarial Compounds

Sandeep Sundriyal[#a], **Nicholas A. Malmquist**[#b,c], **Joachim Caron**[a], **Scott Blundell**[d], **Feng Liu**[e], **Xin Chen**[e], **Nitipol Srimongkolpithak**[a], **Jian Jin**[e,f], **Susan A. Charman**[d], **Artur Scherf**[b,c], and **Matthew J. Fuchter**[*,a]

[a] Department of Chemistry, Imperial College London, London SW7 2AZ, United Kingdom

[b] Unité de Biologie des Interactions Hôte-Parasite, Institut Pasteur, F-75724 Paris CEDEX 15, France

[c] Centre National de la Recherche Scientifique, Unité de Recherche Associée 2581, F-75724 Paris CEDEX 15, France

[d] Monash Institute of Pharmaceutical Sciences, 381 Royal Parade, Parkville, Victoria 3052, Australia

[e] Center for Integrative Chemical Biology and Drug Discovery, Division of Chemical Biology and Medicinal Chemistry, UNC Eshelman School of Pharmacy, University of North Carolina at Chapel Hill, 26 Chapel Hill, North Carolina 27599, United States

[f] Lineberger Comprehensive Cancer Center, University of North Carolina at Chapel Hill, Chapel Hill, North Carolina 27599, United States

[#] These authors contributed equally to this work.

Abstract

Modulating epigenetic mechanisms in malarial parasites is an emerging avenue for the discovery of novel antimalarial drugs. Previously we demonstrated the potent *in vitro* and *in vivo* antimalarial activity of BIX01294 (**1**), a known human G9a inhibitor, together with its dose-dependent effects on histone methylation in the malarial parasite. This work describes our initial medicinal chemistry efforts to optimize the diaminoquinazoline chemotype for antimalarial activity. A variety of analogues were designed by substituting the 2 and 4 positions of the quinazoline core and these molecules were tested against *Plasmodium falciparum* (3D7 strain). Several analogues with IC_{50} values as low as 18.5 nM and with low mammalian cell toxicity (HepG2) were identified. Certain pharmacophoric features required for the antimalarial activity were found to be analogous to the previously published SAR of these analogues for G9a inhibition, thereby suggesting potential similarities between the malarial and the human HKMT

[*] m.fuchter@imperial.ac.uk.

Supporting Information

Supporting information for this article is available on the WWW under http://www.chemmedchem.org or from the author.

targets of this chemotype. Physiochemical, *in vitro* activity, and *in vitro* metabolism studies were also performed for a select set of potent analogues to evaluate their potential as anti-malarial leads.

Keywords

Drug Design; Structure-Activity Relationships; Histone methyltransferase; malaria; diaminoquinazoline

Introduction

Malaria is caused by protozoan parasites belonging to the *Plasmodium* genus (P. falciparum, P. vivax, P. ovale, P. malariae, P. knowlesi) and transferred between human hosts by female *Anopheles* mosquitos. Malaria is prevalent in third world countries and is a major cause of morbidity and mortality, especially in young children and pregnant woman. There were an estimated 207 million cases of malaria, with an estimated 627,000 deaths in 2012.[1] Ninety percent of malaria related deaths occurred in the sub-Saharan African population and 77% occurred in children under the age of five years old. The emergence of multi-drug resistant strains of *Plasmodium*, against which most of the clinically available antimalarial drugs are ineffective, strongly advocates continued efforts in the discovery of novel anti-malarial drugs. [2] Indeed, currently, only artemisnin-based combination therapies (ACTs)[3] offer the most effective way to treat a wide variety of malaria strains, however, reduced sensitivity to artemisinin drugs has now been reported in some areas.[4] Hence, there is need to discover novel targets and more effective drugs which work via a unique mechanism of action in order to control this devastating disease.

Bioinformatic analysis has predicted that, in general terms, the basic transcription machinery in *Plasmodium* is conserved.[5] There is, however, a dearth of knowledge regarding recognizable specific transcription factors in the parasite genome, except for the recent discovery of a family of apicomplexan AP2 transcription factors.[6] In this context, chromatin-mediated epigenetic control has emerged as an important transcriptional mechanism in the complex life cycle of *Plasmodium*.[7] DNA methylation and posttranslational modification (PTM) of histone tails are two of the most commonly studied chromatin modifications that affect epigenetic transcriptional control, and are conserved throughout many diverse species. While there is only one report identifying the DNA methylation in *P. falciparum*,[8] chromatin remodelling through PTM of histones is widely observed.[9] Indeed, it is thought that epigenetic control at the histone PTM level plays a significant role in the transcriptional control of genes encoding proteins implicated in various processes including immune evasion and RBC invasion.[10] Histone lysine acetylation and methylation in particular are found to be predominant in *P. falciparum*. Consequently, the enzymes responsible for these PTMs provide an important opportunity for the discovery of novel antimalarial drugs. In fact, inhibitors of human histone acetyltransferases (HATs) (for example, curcumin or anacardic acid)[11] and the histone deacetylases (HDACs) (for example, nicotinamide, apicidin, or hydroxamic acid derivatives)[12] have been shown to possess antimalarial activity validating acetylation as a useful and novel malarial target.

Recently, we reported the *in vitro* and *in vivo* antimalarial activity of BIX01294 (**1**, Table 1) [13] and a structurally related analogue, in the first effort to validate *Plasmodium* histone lysine methyltransferases (HKMTs) as promising new drug targets.[14] **1** is a known inhibitor of the human HKMTs G9a (EHMT2) and GLP (EHMT1), and was originally discovered by high throughput screening. Analogues based on the diaminoquinazoline scaffold of **1** have been tested against the HKMTs G9a/GLP[15] and structure-activity relationships (SAR) are well understood for G9a/GLP inhibition.[15a-c] In light of the species homology of these important epigenetic targets, we felt this scaffold may be a useful entry into *P. falciparum* HKMT (*Pf*HKMT) inhibitors. Both, **1** and its analogue TM2-115 (**76**, Table 4) were found to inhibit the parasite growth at all stages of the intraerythrocytic life cycle and exhibit a rapid kill effect, positioning this compound class excellently with respect to state of the art experimental antimalarial drugs. Inhibitors **1** and **76** also reduced the overall levels of histone H3K4Me3 of the parasite in dose dependent manner, suggesting the effects observed were related to the proposed *Pf*HKMT target.[13] Recently, it has also been shown that these promising inhibitors can “reawaken” quiescent hepatic hypnozoites, suggesting a potential new means to treat recurrent malaria caused by *P. vivax* infection.[16] In light of these highly promising effects, we set out to explore the initial SAR of diaminoquinazoline analogues for *in vitro* antimalarial activity (3D7 strain of *P. falciparum*) and antiproliferative selectivity between *Plasmodium* and mammalian cell lines.

Chemistry

The first series of compounds were synthesized in two steps starting from the corresponding 2,4-dichloroquinazoline scaffold (Scheme 1). Nucleophilic substitution using the desired amine nucleophile gave access to a 4-substituted quinazoline derivative, that was further heated with a secondary amine under microwave irradiation to afford the target 2,4-diaminoquinazolines, with (Table 1) or without (Table 3) dimethoxy groups at position 6 and 7. Analogues with a *N*-Me group instead of the corresponding *N*-*H* group at position-4 were synthesized by first Boc protecting the amino group of 1-benzylpiperidin-4-amine (**56**) followed by the reduction of carbamate **57** to a secondary amine **58** (Scheme 2). The amine **58** was then installed at position-4 of the 2,4-dichloro-6,7-dimethoxyquinazoline and converted to the final target compounds **60**-**63** as described above (Table 2).

Compounds with an oxygen atom at position-4 were synthesized using 1-benzylpiperidin-4-ol and 2,4-dichloro-6,7-dimethoxyquinazoline in the first step (Scheme 3). This resulted in the isolation of a 4-substituted quinazoline (**64**) which, upon heating with the corresponding amine substrates, yielded target compounds **65** and **66** (Table 2). Compound **72** with a sulphur atom at position-4 was synthesized from *Boc*-protected piperidinol (**67**), which was converted to the desired thiol **68** in three steps (Scheme 4). Analogously, **68** was used to displace chloride at position-4 of 2,4-dichloro-6,7-dimethoxyquinazoline, followed by an acid mediated deprotection of *tert*-butyloxycarbonate group to yield **70**. The ring nitrogen of **70** was then benzylated using reductive amination to afford **71**. Final substitution of this compound with *N*-methyl homopiperazine yielded target compound **72** (Table 2). The analogues bearing 7-*O*-substituted quinazolines described in Table 4 were synthesized using the previously described synthetic route.[15b]

Results and Discussion

In general, our analogue design strategy was cognizant of the interactions of such compounds with G9a/GLP[15a, 15d, 15e, 17], in the absence of *Pf*HKMT structural information. The emerging antimalarial SAR discussed below was therefore compared to known G9a/GLP SAR in order to highlight potential on-target effects against *Pf*HKMTs. The overall important observations from this initial SAR study are summarised in Figure 1.

Initially, the amino substituent at position-2 of our analogues was varied, while fixing a 1-benzyl-4-piperidylamine sidechain at position-4 (Table 1). Decreasing the size of the seven-membered 1-methyl-1,4-diazepine ring of **1** to a comparable six-membered ring slightly improved the antiproliferative *Pf*3D7 activity of the compound (**2**). In fact, a variety of secondary amines were tolerated at position-2 (Entries **3**-**18**, Table 1) without a strong detrimental effect on the potency. Notably, quinazolines substituted with piperidine (**3**), azepane (**4**) and 1-(pyridin-2-yl)piperazine (**5**) were all found to have *Pf*3D7 IC_{50} comparable to **1** (Table 1). This result suggests that position-2 could be used as a handle to fine-tune the physicochemical properties of these inhibitors during lead optimisation studies. Interestingly, such SAR is in accordance with the G9a/GLP activity of the diaminoquinazoline analogues, which tolerates variety of substituents at position-2.[15a-c]

We then sought to vary the substituent at position-4, while fixing key amino substituents at position-2 (Table 1). Substitution of the benzyl group of 4-piperidylamine with a methyl group, led to a reduction in activity by more than 7-fold in the case of **19** *vs* **1** and 16-fold in the case of **20** *vs* **2**. Interestingly however, this effect was not observed when a comparable change was performed in the case of **21** (*vs* **5**), **22** (*vs* **3**) and **23**-**26**. It is plausible therefore that the reduction in activity of **19** and **20** may be due to a physiochemical issue; the benzyl group might be imparting favourable physiochemical properties rather than the controlling on-target potency. This is supported by the fact that clogP values of **19** (2.3) and **20** (1.9) are quite low compared to other highly active molecules such as **1**-**5**, **25** and **26** (clogP ≥ 3.0). Indeed, the *N*-benzyl group of analogues similar to **1** are known to be solvent exposed when bound to GLP (for example, PDB codes 3FPD, 3MO0 and 3MO2),[15d, 17] and therefore replacement of the N-benzyl group with an *N*-methyl group was found not to affect G9a and GLP inhibitory potency.[15a]

One of the important features of substrate competitive HKMT inhibitors such as **1** is the presence of basic functionality, which ensures that the inhibitors are positively charged at physiological pH. This feature is important for long range electrostatic attraction with the negatively charged substrate binding site of the target HKMTs.[18] For our inhibitory series, replacement of the basic nitrogen from the cyclic amine at position-2 with a C-H moiety did not dramatically affect the activity of the compound (Table 1; **1** *vs* **4** and **2** *vs* **3**), however, acylation of the ring basic nitrogen present in the substituent at position-4, thereby decreasing the basicity of this atom, reduced the activity of **27** (*vs* **3**) and **28** (*vs* **5**) by 9-15-fold. Indeed, removal of this particular basic nitrogen (in the position-4 side-chain) was also found to be detrimental for G9a inhibition.[15a] In G9a, this basic centre is within 4.2 Å of the acidic residue Asp1078 (PDB code 3K5K), thus contributing to overall binding, possibly through a charge-assisted hydrogen bond.[15a] Interestingly, sequence alignment of the

*Pf*3D7 SET1 domain (*Pf*SET1) having putative H3K4 methylase activity, with G9a (Fig. S1) suggests this Asp residue to be conserved between the two HKMT proteins.[19] This observation is in agreement with our previous report that treatment of *Pf*3D7 with **1** results in a dose dependent reduction in H3K4 methylation levels in the parasite.[13]

Varying the nature of amine substituent at position-4 led to other interesting observations. Changing the precise positioning of the *N*-Bn moiety (for example, Table 1; **2** *vs* **29** and **5** *vs* **30**) or reducing the size of the piperidine ring (for example, Table 1; **2** *vs* **32**, and **5** *vs* **33**) was found to reduce *Pf*3D7 activity by approximately 4-18-fold. It is possible that such a change in the spatial positioning of the *N*-Bn group may therefore lead to decreased on-target potency. As previously mentioned, installing an acyl group on the basic nitrogen centre was found to decrease the activity by 6-100-fold (for example, Table 1; **21** *vs* **38**, **24** *vs* **41** and **25** *vs* **42**), thus reinforcing the earlier observation that a basic centre is essential at this position. Installing an aniline side-chain at position-4 was also found to reduce the overall activity by 4-31-fold in most cases (for example, Table 1; **2** *vs* **44**, **5** *vs* **45** and **26** *vs* **49**). Furthermore, installation of other structurally diverse amines at position-4, was not successful in improving the potency of our hits. For instance, isopropylamine had a negative effect on the *Pf* antiproliferative activity, reducing potency by 7-17-fold (**1** *vs* **50** and **2** *vs* **51**), which is in agreement with the observed SAR for G9a.[15a] The potency of other analogues with various amine substituent at position-4, such as **52** and **53**, was also reduced by more than 7-fold compared to **1**. Interestingly, with 1-methylpiperidin-4-amine at position-4, analogues containing simple secondary amines at position-2, such as diethylamine (**54**) and dimethylamine (**55**), were found to retain potent activity against *Pf*3D7.

One established piece of SAR of this chemotype against G9a is the need for a free *N-H* functionality at position-4. This functionality forms a hydrogen bond with Asp1083 in the G9a substrate binding pocket, and it is known that masking this functionality with a methyl group results in a significant drop in G9a potency.[15b] Interestingly, *Pf*SET1 has a Ser residue in the analogous position which in theory could form a hydrogen bond with the free *N*-H moiety of such inhibitors (Fig. S1).[19] Indeed, we found the free *N-H* functionality at position-4 was important for the antimalarial activity of this series; replacing it with an *N*-CH_3 group reduced the *Pf*3D7 activity by 10-20-fold, (Table 2; **1** *vs* **60**, **3** *vs* **61**, **4** *vs* **62**, and **5** *vs* **63**). It should be stated, however, that this difference is much less than the ~300-fold drop observed for the activity of the G9a inhibitor UNC0638 upon methylation.[15e] Similarly, replacement of *N*-H with an oxygen or sulphur atom was also found to result in dramatic 100-fold drop in *Pf*3D7 activity (Table 2; **1** *vs* **65**, **5** *vs* **66** and **1** vs **72**).

Next, we sought to explore the 6,7-dimethoxy moiety of this scaffold to better understand the pharmacophoric features of the inhibitors and investigate the potential to add useful substituents to the 6 and 7 position. Removal of both methoxy groups led to a moderate (6-16-fold) decrease in *Pf*3D7 potency (Table 3; **1** *vs* **73, 3** *vs* **74** and **5** *vs* **75**), suggesting that polarity in the 6/7 position has a role in compound activity. To best of our knowledge, such analogues (lacking the 6 and 7 alkoxy groups) have not been reported in terms of their G9a activity, however, no important interactions of 6,7-dimethoxy group with the protein

are obvious in the crystal structure of **1** and other quinazoline analogues in complex with G9a and/or GLP (PDB codes 3K5K, 3RJW, 3FDP, etc.).[15a, 15e, 17] We subsequently investigated derivatives further substituted at positions-7 (Table 4). Our initial study reported a structural isomer of **1**, whereby the terminal benzyl group of the position-4 substituent and the methyl group on the position-7 oxygen atom had been swapped, to give a compound named TM2-115 (**76**, Table 4).[13] We found this isomer to have comparable antimalarial activity to **1**. Clearly, if the benzyl group is removed altogether, and replaced by a methyl group (cf **19**, Table 1) a loss in potency is observed (*vide supra*). Currently, we hypothesise this effect is due to alterations in the overall lipophilicity of the compound (clogP **1** and **76** = 3.86 *vs* clogP **19** = 2.30), rather than through specific interactions with the target.

It is well known that addition of a 'lysine mimic', that is a sidechain that occupies the lysine binding channel of HKMTs, dramatically improves the potency of substrate competitive HKMT inhibitors.[15a, 20] This is due to the improvement in binding strength of such molecules since the 'lysine mimic' makes additional contacts in the lysine binding channel of the protein. In the case of G9a, all optimised (i.e. high potency) analogues reported bear a substituent mimicking a lysine sidechain on the position-7 oxygen atom of the dialkoxydiaminoquinazoline, for example, **78-91** (Table 4).[15a-c] We therefore sought to explore this feature in terms of the antimalarial activity of this series. Thus, 1-methylpiperidin-4-amine and 1-methyl-1,4-diazepine were fixed at position-4 and position-2, respectively, while different lysine mimics were investigated at position-7. Almost all such molecules were found to be inactive indicating that, while such lysine mimics improve G9a/GLP activity, they dramatically decrease the antimalarial activity of this chemotype. It is worth mentioning that many of the tested molecules in this series had lower clogP such as, **78**, **83**, and **87** and/or higher topological polar surface area such as **87-89** due to the additional polar functionality in the *O*-7 sidechain. Analogues such as **90** and **91**, with less polar lysine mimics did exhibit moderate activity. Hence, the negative effect of the extended *O*-7 substituents on the antimalarial activity of this compound class might be due to their poor permeability as suggested previously.[15c] Alternatively, it is plausible that the lysine binding channel within the malarial parasite HKMT target is not comparable to the corresponding channel in G9a. Indeed, a recent computational comparison of various SET domain containing methyltransferases has revealed that residues in the lysine binding channel are surprisingly diverse and that a single chemical 'lysine mimic' scaffold will likely not fit optimally, nor satisfy the varied distribution of binding hotspots across a range of HKMTs.[20]

Whilst, in the absence of structural *Pf*HKMT information or enzymatic *Pf*HKMT activity data, we have related the *Pf*3D7 SAR obtained to SAR observed for this compound class against human G9a/GLP, it will ultimately be important to diverge from human target (and off target) activity in the development of an optimised anti-malarial lead compound for progression to clinical candidacy. We therefore assessed representative compounds for cytotoxicity against the human HepG2 hepatocarcinoma cell line as a measure of parasite versus human selectivity (see Table 1). Promisingly, our lead compounds **1**, **76**, **11** and **22** were found to not only be highly potent against *Pf*3D7, but also highly selective for parasite

versus host cell killing (Table 5).[21] All four compounds were found to be 110-388-fold more active on *Pf*3D7 compared to HepG2 cell viability. Hence, these molecules were selected for further *in vitro* activity, physiochemical and *in vitro* metabolism studies.

We previously showed **1** and **76** to exhibit a fast killing phenotype effective throughout the intraerythrocytic parasite life cycle.[13] Killing phenotypes are a function of the parasite molecular target, and as such, we tested compounds **11** and **22** for a similar phenotype in an effort to demonstrate continued on-target killing as we develop our diaminoquinazoline series. Treating highly synchronized parasites for three distinct periods of the 12-hour intraerythrocytic stage and quantifying re-invasion into the next cycle or out-growth two cycles later reveals both **11** and **22** to possess a similar rapid and erythrocytic stage-independent killing phenotype (Figure 2) as previously shown for **1** and **76**.[13] As measured by flow cytometry, parasite re-invasion appears greatly reduced (Figure 2b), though Giemsa-stained blood smears reveal these counted parasites to likely be dead parasites from the previous cycle (data not shown). Treated and washed parasites allowed to grow in the absence of compound for an additional two cycles show virtually no parasite survival after a 12-hour treatment with either compound **11** or **22** regardless of the phase of the intraerythrocytic cycle in which they were treated (Figure 2c).

To further investigate the mechanism of action of **11** and **22** we treated parasites for 12 hours with 5-fold IC_{50} concentrations **1**, **11**, **22**, and chloroquine and estimated histone H3K4me3 and H3K9me3 levels by Western blot (Figure 3) in treated parasites relative to control parasites treated with DMSO vehicle. We previously demonstrated a decrease in H3K4me3 and H3K9me3 levels upon treatment of parasites with **1**.[13] The data reveal decreased H3K4me3 and H3K9me3 levels in parasites treated with 5-fold IC_{50} concentrations **1**, **11**, **22**. Parasites treated similarly with chloroquine, an established antimalarial with a fast killing profile, show a slight decrease in H3K4me3 and a slight increase in H3K9me3 levels. These data further support the hypothesis that **11** and **22** target the same molecular mechanism as **1**, namely parasite histone methyltransferases. Our previous report that **1** is equally potent against both chloroquine-sensitive and chloroquine-resistant parasites[13] additionally support the notion that diaminoquinazolines from this series and 4-amino quinolines such as chloroquine operate through distinct mechanisms.

The measured distribution coefficient (logD) values for all four compounds were shown to be pH dependent suggesting changes in ionisation occurring between pH 7.4 and 3. The observed changes are consistent with compound **1** and **76** being tri-basic and **11** and **22** being di-basic. At pH 6.5, all compounds demonstrated good aqueous solubility (≥ 50 μg/mL) except **22** which possessed only moderate solubility (6.3-12.5 μg/mL). As would be expected for such basic compounds, the solubility of all compounds improved at pH 2. Various assays were conducted to determine the *in vitro* metabolic stability of these molecules (Table 5). After 4 hour incubation in rat plasma, all four compounds remained within ±15% of the initial value therefore demonstrating good plasma stability. The inhibitors exhibited low to intermediate rates of degradation in rat liver microsomes with $t_{1/2}$ values ranging from 28 to 184 minutes and *in vitro* intrinsic clearance values (CL_{int}) ranging from 9-62 μl/min/mg protein. Additionally, no measurable degradation of any of the compounds in microsomal matrix was observed in the absence of cofactor (control

incubations, data not shown), suggesting that there was no major non-cofactor dependent metabolism contributing to the overall rates of metabolism.

These results together with the predicted hepatic extraction ratio (E_H, Table 5) suggest that **11**, bearing a ring with a methoxy substituent at position-2, is the most metabolically stable analogue among the four molecules. This is in accordance with a recent study reporting that a substitution on piperidyl ring at position-2 might prevent CYP450 mediated *in vitro* oxidation of this position.[22] The role of position-2 substituent in governing the overall stability is further corroborated by the fact that **1** and **2** have a metabolically labile *N*-Me moiety at this position and are correspondingly less stable. Expectedly, **22** lacking an *N*-Me moiety in the aforementioned position, but also lacking substitution on piperidyl ring exhibits intermediate stability.

Conclusions

In summary we have designed and synthesized analogues of a reported human HKMT G9a and GLP inhibitor (**1**), which we previously reported to have potent antimalarial activity. The aim of this study was to better define SAR with respect to the antimalarial activity of this chemotype. Many of the analogues prepared were found to possess potent antimalarial activity against *P. falciparum*, in the nanomolar range and exhibited selectivity over human HepG2 cells. Initial SAR analysis has indicated that most of the structural requirements for malarial activity were common to human G9a activity, as may be expected for on-target activity against a homologous *Pf*HKMT enzyme. For example, a basic centre within the cyclic amine at position-4 was found to be crucial for compound potency, suggesting the inhibitor-protein interaction (with Asp1078 for G9a) may be conserved upon moving from a human to a *P. falciparum* HKMT. Similarly, an available *N*-H moiety at position-4 was also found to be a key feature, as is the case for G9a inhibitors belonging to this chemotype. A variety of diverse secondary amine sidechains could be installed at position-2 without dramatically affecting the *Pf*3D7 activity, which again is in agreement with G9a SAR. Conversely however, the presence of a ‘lysine mimic’ side-chain at position-7, central for highly potent G9a inhibition, was found to abolish the antimalarial activity of this series. While partially explained by the reduced clogP, and thereby permeability of such analogues in our cell based assay, it is plausible that the presumed target *Pf*HKMT lysine binding channel possesses a dissimilar ‘hotspot’ profile to G9a/GLP.[20] Finally, further *in vitro* activity, physiochemical and *in vitro* metabolism studies of lead molecules emerging from this series were carried out. All leads exhibited the same killing phenotype and were found to decrease the H3K4me3 and H3K9me3 levels in treated parasites, supporting the hypothesis of diaminoquinazolines targeting one or more parasite HKMT. A substituent at position-2 was found to be important for the overall *in vitro* metabolic stability of the compounds in this series. Overall, this study will aid in the further optimisation of this compound class as future antimalarial drug candidates.

Experimental Procedures

In vitro P. falciparum growth and proliferation assays

Compounds were tested against drug sensitive *P. falciparum* 3D7 strain parasites using a three-day SYBR Green I based assay.[23] Parasites were cultured at 2% hematocrit with an initial parasitemia of 0.5-0.8% in RPMI 1640 containing 0.5% albumax. Compounds were initially screened at 2 μM in duplicate wells in a 96-well format. Subsequent IC_{50} values for active compounds were determined with 2:1 dilutions of test compounds.

In vitro cytotoxicity assays

Host cell cytotoxicity was determined in a 96-well format with a starting HepG2 cell density of 10000 cells/well grown in DMEM. Cells were incubated with 1:1 dilutions of test compounds for three days and resulting cell viability was quantified using Promega CellTiterBlue.

In vitro stage-dependent antimalarial activity

Stage-specific compound treatment effects were elucidated using highly synchronized parasites in 48-well plates with a starting parasitemia of 0.75% and a hematocrit of 2%. Parasites were treated for 12 hours with 10x IC_{50} concentrations of compounds **11** or **22** during three distinct periods of the intraerythrocytic life cycle. After treatment, parasites were washed with warm RPMI 1640 medium and placed back into culture without test compound for analysis of re-invasion after completion of the cell cycle in which treatment occurred.

Washed parasites after treatment were also diluted 1:16 and allowed to grow without compound for an additional two cell cycles (4 days). Parasitemia after re-invasion or after 4-day growth was quantified on infected cells fixed in 0.25% glutaraldehyde and stained with 2x SYBR Green I (Invitrogen) in PBS.

Parasite histone methlyation analysis

*P. falciparum*3D7 strain parasites were treated for 12 hours with **1**, **11**, **22** or chloroquine (CQ), infected blood was collected, treated with 0.15% saponin in PBS to lyse and remove red blood cells, then free parasites were lysed by bath sonication in 2% SDS and subjected to Western blot analysis. Blots were probed with specific primary antibodies for histone H3 core (Abcam ab1792, 1:5000), histone H3K4me3 (Abcam ab1020, 1:1000) or histone H3K9me3 (Abcam ab8898, 1:1000) diluted in TBS-T (50 mM Tris pH 7.5, 150 mM NaCl, 0.25% gelatin, 0.05% Tween-20), followed by anti-mouse HRP (GE NXA931) or anti-rabbit HRP (GE NA-934) secondary antibodies. Blots were revealed using Pierce SuperSignal West Pico chemiluminescent substrate and quantified using Bio-Rad Image Lab software.

clogP and TPSA calculation

These physicochemical properties were calculated using RDKit which is an open-source cheminformatics toolkit.[24]

In vitro solubility, log D and metabolic stability studies

These studies were performed at the Center for Drug Candidate Optimization (CDCO), Monash Institute of Pharmaceutical Sciences, Monash University, Australia. Kinetic solubility was assessed at pH 2 and 6.5 using nephelometry, and Log D was estimated at pH 3 and 7.4 using a chromatographic method; both of these methods have been described previously.[25]

Metabolic stability was assessed by incubating the test compounds in rat liver microsomes (Xenotech, Lenexa, KS) at 37°C using a substrate concentration of 1 μM and a microsomal protein concentration of 0.4 mg/mL. The metabolic reaction was initiated by the addition of an NADPH-regenerating system and quenched at various time points over 60 minutes using chilled acetonitrile. Additional control samples were incubated in the absence of NADPH to monitor for non-cytochrome P450 dependent metabolism. Samples were centrifuged at 4600 rpm for 3 minutes on a Heraeus Multifuge 3 S-R centrifuge before a 5 μL injection of the supernatant was analysed by LC/MS.

LC/MS analysis was conducted on a Waters/Micromass Quattro Ultima PT Triple Quadrupole MS coupled to a Waters Acquity UPLC (Milford, MA) under positive electrospray ionisation.

Chromatography was conducted using an Ascentis Express RP-Amide column (50x2.1 mm, 2.7 μm) (Sigma-Aldrich, St Louis, MO) equipped with a Phenomenex SecurityGuard column and a Luna C8 cartridge (Torrance, CA) and both were maintained at a temperature of 40 °C. The mobile phase consisted of an aqueous phase (0.05% formic acid) and acetonitrile. A 4-minute binary gradient was employed for optimum elution of the analyte and internal standard (75 ng/mL Diazepam).

The first-order rate constant for substrate depletion was used to calculate the *in vitro* intrinsic clearance which was scaled to predict the *in vivo* intrinsic clearance as described previously.[26] The blood clearance and the predicted hepatic extraction ratio (EH) were calculated using the well-stirred model of hepatic clearance based on scaling factors and hepatic blood flow that have been d reported previously.[27]

Chemistry General Procedures—All reactions were performed under an atmosphere of dry nitrogen unless otherwise stated. Reagents were obtained from commercial suppliers or redistilled if required. Flash column chromatography was carried out using Merck Kiesegal 60 silica gel (230-400 mesh). Compounds **6**-**18** and **21**-**49** (Table 1) were prepared by contract synthesis at SAI Life Sciences Limited and their data is reported in the supporting information. Synthetic methodology and spectrometric data for compounds **19**, **20**, **50**, **52**-**55** (Table 1) and **76**-**92** (Table 4) was described previously.[15a-c] All compounds evaluated in biological assays had >95% purity as judged by the HPLC or LCMS.

Synthetic methodology

(1-Benzyl-4-piperidyl)[6,7-dimethoxy-2-(4-methyl-1,4-diazepin-1-yl)-4-quinazolinyl]amine (1, BIX01294)—A mixture of N-(1-benzylpiperidin-4-yl)-2-chloro-6,7-dimethoxyquinazolin-4-amine (0.413 g, 1 mmol) which was prepared according

to the procedures described previously,[15a] and 1-methyl-1,4-diazepane (0.6 mL, 5 mmol) in 2 mL toluene was heated at 130 °C for 50 minutes under microwave irradiation. The reaction mixture was concentrated and purified by silica gel column chromatography using MeOH (7 N NH_3) and DCM gradient (2-5% of MeOH). The title product was obtained as light yellow solid (0.489 g, 79 %).^{1}H NMR (400 MHz, $CDCl_3$) δ 7.34-7.23 (m, 5H), 6.89 (s, 1H), 6.69 (s, 1H), 4.96 (d, *J* = 7.8 Hz, 1H), 4.15-4.06 (m, 1H), 3.99-3.96 (m, 2H), 3.95 (s, 3H), 3.92 (s, 3H), 3.88 (t, *J* = 6.4 Hz, 2H), 3.55 (s, 2H), 2.92-2.89 (m, 2H), 2.71-2.69 (m, 2H), 2.58-2.56 (m, 2H), 2.37 (s, 3H), 2.22-2.13 (m, 4H), 2.04-1.98 (m, 2H), 1.62 (qd, *J* = 11.6, 11.0, 4.0 Hz, 2H); MS (ESI) *m/z* 491 $[M+H]^+$; HRMS (ESI) *m/z* $[M+H]^+$ calcd for $C_{28}H_{39}N_6O_2$: 491.3134, found: 491.3124.

Compounds no. **2-5, 51**, **73-75** (Table 1) were synthesized following an analogous approach as for **1** with the following spectroscopic data:

(1-Benzyl-4-piperidyl)[6,7-dimethoxy-2-(4-methyl-1-piperazinyl)-4-quinazolinyl]amine (2)—^{1}H NMR (400 MHz, $CDCl_3$): δ 7.34-7.27 (m, 5H), 6.90 (s, 1H), 6.70 (s, 1H), 5.02 (d, *J* = 7.2 Hz, 1H), 4.19–4.09 (m, 1H), 3.94 (s, 3H), 3.92 (s, 3H), 3.86 (m, 4H), 3.55 (s, 2H), 2.91 (m, 2H), 2.49 (m, 4H), 2.34 (s, 3H), 2.21 (m, 2H) 2.15 (m, 2H), 1.62 (qd, *J* = 2.9, 11.5 Hz, 2H); HRMS (ESI) *m/z* $[M+H]^+$ calcd. for $C_{27}H_{37}N_6O_2$, 477.2978; found: 477.2970.

(1-Benzyl-4-piperidyl)(6,7-dimethoxy-2-piperidino-4-quinazolinyl)amine (3)—^{1}H NMR (400 MHz, $CDCl_3$): δ 7.34-7.24 (m, 5H), 6.90 (br s, 1H), 6.68 (s, 1H), 4.95 (br s, 1H), 4.19–4.09 (m, 1H), 3.95 (s, 3H), 3.93 (s, 3H), 3.80 (m, 4H), 3.55 (s, 2H), 2.91 (m, 2H), 2.21 (m, 2H) 2.15 (m, 2H), 1.64 (m, 8H); HRMS (ESI) *m/z* $[M+H]^+$ calcd. for $C_{27}H_{36}N_5O_2$, 462.2868; found: 462.2855

(1-Benzyl-4-piperidyl)[2-(1-azepinyl)-6,7-dimethoxy-4-quinazolinyl]amine (4)—^{1}H NMR (400 MHz, CD_3OD) δ 7.43 (s, 1H), 7.36-7.28 (m, 5H), 6.90 (s, 1H), 4.18-4.16 (m, 1H), 3.91 (s, 3H), 3.89 (s, 3H), 3.77 (t, *J* = 12.0, 4H), 3.58 (s, 2H), 3.01 (d, *J* = 12.0, 2H), 2.18 (t, *J* =12.0, 2H), 2.09 (d, *J* = 12.0, 2H), 1.82-1.73 (m, 6H), 1.31- 1.29 (m, 4H) ;HRMS (ESI) *m/z* calc. for $C_{28}H_{42}N_5O_2$,476.3026; found: 476.3061.

(1-Benzyl-4-piperidyl){6,7-dimethoxy-2-[4-(2-pyridyl)-1-piperazinyl]-4-quinazolinyl}amine (5)—^{1}H NMR (400 MHz, CD_3OD): δ 8.16 (m, 1H), 7.76 (br s, 1H), 7.62 (m, 3H), 7.51 (m, 3H), 7.19 (br s, 1H), 6.92 (m, 1H), 6.75 (m, 1H), 4.62 (m, 1H), 4.34 (br s, 2H), 4.04 (m, 4H), 3.98 (s, 3H), 3.96 (s, 3H), 3.77 (m, 4H), 3.57 (br *app*-d, *J* = 12.4 Hz, 2H), 3.30 (m, 2H), 2.34 (br *app*-d, *J* = 12.6 Hz, 2H), 2.17 (m, 2H); HRMS (ESI) *m/z* $[M+H]^+$ calcd. for $C_{31}H_{38}N_7O_2$, 540.3087; found: 540.3077

(1-Benzyl-4-piperidyl)[2-(4-methyl-1,4-diazepin-1-yl)-4-quinazolinyl]amine (73)—^{1}H NMR (400 MHz, CD_3OD) δ 7.95 (d, *J* = 7.2 Hz, 1H), 7.52 (t, *J* = 8.0 Hz, 1H), 7.41 (d, *J* = 8.0 Hz, 1H), 7.34-7.13 (m, 5H), 7.11 (t, *J* = 7.2 Hz, 1H), 5.42 (br.S, 1H), 4.18-4.09 (m, 1H), 3.96 (t, *J* = 4.8 Hz, 2H), 3.86 (t, *J* = 5.6 Hz, 2H), 3.57 (s, 2H), 2.97(d, *J* =12.0Hz, 2H), 2.88 (t, *J* =4.8Hz, 2H),2.74 (t, *J* =5.6Hz, 2H), 2.49(s, 3H), 2.04 (t, *J* = 12.0 Hz, 2H),

2.06-2.03 (m, 4H), 1.72 (dq, *J* = 12.0, 3.2 Hz, 2H) ; MS (ESI) m/*z* 431.3 $[M+H]^+$. HRMS *m/z* $[M+H]^+$ calcd. for $C_{26}H_{35}N_6$, 431.2903; found: 431.2923.

(1-Benzyl-4-piperidyl)(2-piperidino-4-quinazolinyl)amine (74)—^{1}H NMR (400 MHz, $CDCl_3$) δ 7.95-7.94 (d, *J* = 7.2, 1H), 7.56-7.52 (t, *J* = 8.0, 1H), 7.49 (d, *J* = 12.0, 1H), 7.34-7.23 (m, 5H), 7.14 (t, *J* = 12.0, 1H), 4.18-4.08 (m, 1H), 3.80 (t, *J* = 5.6, 4H), 3.56 (s, 2H), 2.98 (d, *J* = 12.0, 2H), 2.19 (t, *J* = 12.0, 2H), 2.05 (d, *J* = 12.0, 2H), 1.77-1.62 (m, 8H); MS (ESI) *m/z* 402.3 $[M+H]^+$.

(1-Benzyl-4-piperidyl){6,7-dimethoxy-2-[4-(2-pyridyl)-1-piperazinyl]-4-quinazolinyl}amine (75)—^{1}H NMR (400 MHz, MeOD) δ 8.10 (d, *J* = 4.8, 1H), 7.93 (d, *J* = 8.0, 1H), 7.60-7.51 (m, 2H), 7.41-7.26 (m, 6H), 7.09 (t, *J* = 8.0, 1H), 6.84 (br, d, 8.0, 2H), 6.69 (m, 1H), 4.20-4.17 (m, 1H), 3.97 (br, s, 4H), 3.59 (br, s, 6H), 2.99 (d, *J* = 10.0, 2H), 2.24 (t, *J* = 10.0, 2H), 2.08 (d, *J* = 12.0, 2H), 1.73 (quin, *J* = 12.0, 2H); MS (ESI) *m/z* 480.4 $[M+H]^+$.

(Isopropyl)[6,7-dimethoxy-2-(4-methyl-1-piperazinyl)-4-quinazolinyl]amine (51)—To a solution of (Isopropyl)(2-chloro-6,7-dimethoxy-4-quinazolinyl)amine (263 mg, 0.93 mmol) which was prepared according to the procedures described previously,[15b] in 4 mL of *i*-PrOH was added 1-methylpiperazine (0.21 mL, 1.86 mmol), followed by 0.47 mL of HCl in dioxane (4.0 M, 1.86 mmol). The resulting mixture was then stirred at 160 °C under microwave irradiation for 15 minutes. After the addition of 1 mL NH_4OH, the solvent was removed and the residue was subjected to flash chromatography purification to give the desired compound as off-white solid (234 mg, 73%). ^{1}H NMR (400 MHz, CD_3OD) δ 7.40 (s, 1H), 6.87 (s, 1H), 4.49 (dt, *J* = 13.2, 6.6 Hz, 1H), 3.90 (s, 3H), 3.89 (s, 3H), 3.87 – 3.78 (m, 4H), 2.56 – 2.48 (m, 4H), 2.34 (s, 3H), 1.32 (d, *J* = 6.6 Hz, 6H). MS (ESI) *m/z* 346.25 $[M+H]^+$.

***tert*-butyl (1-benzylpiperidin-4-yl)carbamate (57)—**To a solution of 1-benzylpiperidin-4-amine **56** (1 mL, 933 mg, 4.9 mmol) in dry DCM (20 mL) were added Et_3N (1 mL, 725 mg, 7.2 mmol) and di-*tert*-butyl dicarbonate (1.23 g, 5.6 mmol). The reaction mixture was stirred overnight at room temperature and then diluted with DCM (20 mL). The organic layer was washed with aqueous $NaHCO_3$ solution and brine, dried over anhydrous $MgSO_4$ and concentrated *in vacuo* to give **57** (1.42 g, quant.) as a white solid. ^{1}H NMR (400 MHz, $CDCl_3$) δ 7.37-7.28 (m, 4H), 7.27-7.22 (m, 1H), 4.45 (br, s, 1H), 3.48 (s, 2H), 2.79 (br, d, *J* = 11.8 Hz, 2H), 2.08 (td, *J* = 11.8, 2.0 Hz, 2H), 1.89 (d, *J* = 11.8 Hz, 2H), 1.47-1.37 (m, 11H).

***N*-Methyl(1-benzyl-4-piperidyl)amine (58)—**To a suspension of $LiAlH_4$ (1.0 g, 26.35 mmol) in dry THF (10 mL), was added dropwise at 0 °C a solution of **57** (1.4 g, 4.82 mmol) in dry THF (10 mL). The reaction mixture was refluxed for 72 hours, cooled to 0 °C and diluted with THF. Ethyl acetate was added to quench the excess of $LiAlH_4$ and 3*N* aqueous NaOH solution was added to form a white precipitate. The mixture was filtrated over a celite cake and the filtrate was concentrated under reduced pressure to furnish **58** (980 mg, quant.)

as a pale yellow oil. Crude product was engaged in the next reaction without further purification.

(1-Benzyl-4-piperidyl)-*N*-methyl(2-chloro-6,7-dimethoxy-4-quinazolinyl)amine (59)—To a mixture of 2,4-dichloro-6,7-dimethoxyquinazoline (650 mg, 2.51 mmol) and **58** (680 mg, 3.34 mmol) in dry THF (16 mL) was added Et_3N (1.4 mL, 1.02 g, 10.0 mmol). The reaction mixture was stirred overnight at room temperature and then concentrated under reduced pressure. The residue was purified by flash chromatography (DCM/MeOH 100:0 to 98:2) to furnish **59** (500 mg, 47%) as a white solid. ^{1}H NMR (400 MHz, $CDCl_3$) δ 7.35-7.30 (m, 4H), 7.28-7.24 (m, 1H), 7.14 (s, 1H), 7.12 (s, 1H), 4.29 (tt, *J* = 10.8 Hz, 3.7 Hz, 1H), 3.98 (s, 3H), 3.93 (s, 3H), 3.53 (s, 2H), 3.17 (s, 3H), 3.03 (d, *J* = 10.8 Hz, 2H), 2.15-1.97 (m, 4H), 1.90-1.83 (m, 2H).

(1-Benzyl-4-piperidyl)-*N*-methyl[6,7-dimethoxy-2-(4-methyl-1,4-diazepin-1-yl)-4-quinazolinyl]amine (60)—To a solution of **59** (63 mg, 0.15 mmol) in dry toluene (3 mL) was added 1-methyl-1,4-diazepane (0.18 mL, 165 mg, 1.45 mmol). The reaction mixture was refluxed overnight and then concentrated under reduced pressure. The residue was purified by flash chromatography (DCM/MeOH 97:3 to 95:5) to furnish quinazoline **12d** (48 mg, 63%) as colourless oil. ^{1}H NMR (400 MHz, CD_2Cl_2) δ 7.34-7.29 (m, 4H), 7.28-7.21 (m, 1H), 7.04 (s, 1H), 6.85 (s, 1H), 4.19-4.08 (m, 1H), 3.95-3.89 (m, 5H), 3.86-3.81 (m, 5H), 3.49 (s, 2H), 3.08 (s, 3H), 2.99 (br, d, *J* = 10.0 Hz), 2.71-2.66 (m, 2H), 2.58-2.52 (m, 2H), 2.34 (s, 3H), 2.10-1.92 (m, 6H), 1.88-1.81 (m, 2H). MS (ESI) *m/z* 505.3 $[M+H]^+$. HRMS (ESI) *m/z* $[M+H]^+$ calcd for C $^{29}H_{41}N_6O_2$: 505.3291, found: 505.3277.

Compound **61**-**63** were synthesized following procedure similar to **60**

(1-Benzyl-4-piperidyl)-*N*-methyl(6,7-dimethoxy-2-piperidino-4-quinazolinyl)amine (61)—^{1}H NMR (400 MHz, $CDCl_3$)δ 7.35-7.30 (m, 4H), 7.29-7.23 (m, 1H), 7.01 (s, 1H), 6.94 (br, s, 1H), 4.19-4.07 (m, 1H), 3.96 (s, 3H), 3.88 (s, 3H), 3.82-3.78 (m, 4H), 3.51 (s, 2H), 3.07 (s, 3H), 3.05-2.99 (m, 2H), 2.10-1.95 (m, 4H), 1.89-1.83 (m, 2H), 1.70-1.58 (m, 6H). MS (ESI) *m/z* 476.3 $[M+H]^+$. HRMS (ESI) *m/z* $[M+H]^+$ calcd for $C_{28}H_{38}N_5O_2$: 476.3026, found: 476.3028.

(1-Benzyl-4-piperidyl)-*N*-methyl[2-(1-azepinyl)-6,7-dimethoxy-4-quinazolinyl]amine (62)—^{1}H NMR (400 MHz, CD_2Cl_2) δ 7.35-7.29 (m, 4H), 7.28-7.22 (m, 1H), 7.09 (br, s, 1H), 7.05 (s, 1H), 4.21 (br, t, *J* = 10.3 Hz), 3.93 (s, 3H), 3.84 (s, 3H), 3.80 (b, t, *J* = 5.7 Hz) 3.49 (s, 2H), 3.12 (s, 3H), 3.00 (br, d, *J* = 11.2 Hz), 2.11-1.92 (m, 4H), 1.89-1.75 (m, 6H), 1.58-1.51 (m, 4H). MS (ESI) *m/z* 490.3 $[M+H]^+$. HRMS (ESI) *m/z* $[M+H]^+$ calcd for $C_{29}H_{40}N_5O_2$: 490.3182, found: 490.3167.

(1-Benzyl-4-piperidyl)-*N*-methyl{6,7-dimethoxy-2-[4-(2-pyridyl)-1-piperazinyl]-4-quinazolinyl}amine (63)—^{1}H NMR (400 MHz, CD_2Cl_2) δ 8.17 (ddd, *J* = 4.9 Hz, 2.0 Hz, 0.80 Hz, 1H), 7.50 (m, 1H), 7.35-7.29 (m, 4H), 7.28-7.22 (m, 1H), 7.06 (s, 1H), 6.89 (s, 1H), 6.71 (d, *J* = 8.6 Hz, 1H), 6.62 (ddd, *J* = 7.1 Hz, 4.9 Hz, 0.80 Hz, 1H), 4.18 (tt, *J* = 11.2 Hz, 3.8 Hz, 1H), 3.94-3.90 (m, 7H), 3.85 (s, 3H) 3.63-3.58 (m, 4H), 3.50 (s, 2H), 3.11 (s, 3H),

3.00 (br d, J = 11.2 Hz), 2.17-1.94 (m, 4H) 1.90-1.83 (m, 2H). MS (ESI) *m/z* 554.3 $[M+H]^+$. HRMS (ESI) *m/z* $[M+H]^+$ calcd for $C_{32}H_{40}N_7O_2$: 554.3243, found: 554.3237.

4-(1-Benzyl-4-piperidyloxy)-2-chloro-6,7-dimethoxyquinazoline (64)—To a mixture of 2,4-dichloro-6,7-dimethoxyquinazoline (515 mg, 2.0 mmol) and 1-benzylpiperidin-4-ol (430 mg, 2.25 mmol) in dry DMSO (7.5 mL) was added slowly at room temperature KO*t*-Bu (335 mg, 3.0 mmol). The reaction mixture was stirred at room temperature for 2 hours. Water (20 mL) was added and the aqueous layer was extracted with DCM (3 × 30 mL). The combined organic extracts were washed with brine (30 mL), dried over anhydrous $MgSO_4$ and then concentrated under reduced pressure. The crude product was purified by flash chromatography (EtOAc/Pet. Ether 1:1) to furnish the title compound **64** (550 mg, 67%) as a pale yellow solid. ^{1}H NMR (400 MHz, $CDCl_3$) δ 7.36-7.29 (m, 4H), 7.28-7.22 (m, 2H), 7.17 (s, 1H) 5.41 (tt, J = 8.2 Hz, 4.0 Hz, 1H, H_3), 3.99 (s, 3H), 3.98 (s, 3H), 3.57 (s, 2H), 2.85-2.75 (m, 2H), 2.40 (br, t, J = 9.1 Hz), 2.18-2.09 (m, 2H), 2.00-1.90 (m, 2H)

4-(1-Benzyl-4-piperidyloxy)-6,7-dimethoxy-2-(4-methyl-1,4-diazepin-1-yl)quinazoline (65)—To a solution of **64** (80 mg, 0.19 mmol) in dry toluene (3 mL) was added 1-methyl-1,4-diazepane (0.25 mL, 230 mg, 2.0 mmol). The reaction mixture was refluxed overnight and then concentrated under reduced pressure. The residue was purified by flash chromatography (DCM/MeOH 99:1 to 95:5) to furnish quinazoline **65** (87 mg, 93%) as a yellow oil. ^{1}H NMR (400 MHz, $CDCl_3$) δ 7.37-7.31 (m, 4H), 7.29-7.23 (m, 1H), 7.17 (s, 1H), 6.89 (s, 1H), 5.28 (dq, J_1 = 11.8 Hz, 3.8 Hz, 1H), 3.99-3.95 (m, 5H), 3.93 (s, 3H), 3.87(t, J = 6.4 Hz, 2H), 3.57 (s, 2H), 2.83-2.70 (m, 4H), 2.62-2.56 (m, 2H), 2.41-2.35 (m, 5H), 2.14-2.03 (m, 4H), 2.00-1.99 (m, 2H). MS (ESI) *m/z* 492.3 $[M+H]^+$. HRMS (ESI) *m/z* $[M+H]^+$ calcd for $C_{28}H_{38}N_5O_3$: 492.2975, found: 492.2965.

4-(1-Benzyl-4-piperidyloxy)-6,7-dimethoxy-2-[4-(2-pyridyl)-1-piperazinyl]quinazoline (66)—66 was synthesized following a procedure similar to **65**. ^{1}H NMR (400 MHz, $CDCl_3$) δ 8.22 (ddd, J = 4.9 Hz, 1.9 Hz, 0.68 Hz, 1H), 7.50 (m, 1H), 7.37-7.30 (m, 4H), 7.29-7.23 (m, 1H), 7.19 (s, 1H), 6.94 (s, 1H), 6.70 (d, J = 8.60 Hz, 1H), 6.64 (m, 1H), 5.30 (m, 1H), 3.98-3.94 (m, 10H), 3.66-3.64 (m, 4H), 3.58 (s, 2H), 2.85-2.76 (m, 2H), 2.52-2.46 (m, 4H), 2.39 (t, J = 8.8 Hz, 2H), 2.17-2.09 (m, 2H), 2.00-1.91 (m, 2H). MS (ESI) *m/z* 541.3 $[M+H]^+$. HRMS (ESI) *m/z* $[M+H]^+$ calcd for $C_{31}H_{37}N_6O_3$: 541.2927, found: 541.2936.

2-Chloro-6,7-dimethoxy-4-(4-piperidylthio)quinazoline (70)—To a suspension of sodium hydride (60% in mineral oil, 70 mg, 1.75 mmol) in dry THF (4 mL) was added dropwise at 0 °C, a solution of thiol **69** (350 mg, 1.61 mmol) in dry THF (4 mL). Reaction mixture was stirred at 0 °C for 20 minutes and a solution of 2,4-dichloro-6,7-dimethoxyquinazoline (415 mg, 1.60 mmol) in dry THF (4 mL) was added dropwise. The mixture was stirred for 1 hour at 0 °C and then overnight at room temperature. An aqueous ammonium chloride solution (20 mL) was added and the aqueous phase was extracted with diethyl ether (2×50 mL). The combined organic extracts were washed with brine (40 mL), dried over anhydrous $MgSO_4$ and concentrated under reduced pressure. The crude product

was purified by flash chromatography (Petroleum Ether/Et_2O 2:1 to 1:1) to furnish 4-thioquinazoline **69** (560 mg, 80%) as a colourless solid. Compound **69** (170 mg, 0.39 mmol) was solubilised in 4N HCl solution in dioxane (5 mL, 20 mmol). The reaction mixture was stirred overnight at room temperature and then concentrated under reduced pressure to give hydrochloride salt of piperidine **70** (170 mg, 98%) as a light brown solid.

^{1}H NMR (400 MHz, d_6-DMSO) δ 9.38 (br, s, 1H), 9.17 (br, s, 1H), 7.67 (br, s, 2H), 7.31 (s, 1H), 7.16 (s, 1H), 4.26 (td, *J* = 10.4, 5.1 Hz, 1H), 3.96 (s, 3H), 3.94 (s, 3H), 3.30 (br, d, *J* = 12.8 Hz, 2H), 3.13 (br, q, *J* = 12.8 Hz, 2H), 2.30 (dd, *J* = 12.8, 3.2 Hz, 2H), 2.00 (qd, *J* = 12.8, 3.2 Hz, 2H). MS (ESI) *m/z* 340.1 $[M+H]^+$. HRMS (ESI) *m/z* $[M+H]^+$ calcd for $C_{15}H_{18}ClN_3O_2S$: 340.0887, found: 340.0882.

4-(1-Benzyl-4-piperidylthio)-2-chloro-6,7-dimethoxyquinazoline (71)—To a solution of **70** (170 mg, 0.38 mmol) in an ethanol/methylene chloride mixture (10 : 5 mL) were added triethylamine (0.16 mL, 1.19 mmol), acetic acid (0.07 mL, 1.22 mmol) and then benzaldehyde (0.06 mL, 0.59 mmol). The reaction mixture was stirred for 5 minutes and sodium triacetoxyborohydride (130 mg, 0.60 mmol) was added. The reaction mixture was stirred overnight at room temperature and then concentrated under reduced pressure. The crude residue was purified by flash chromatography (DCM/MeOH 100:0 to 98:2) to give *N*-benzylpiperidine **71** (110 mg, 67%) as a yellow oil. ^{1}H NMR (400 MHz, CD_3OD) δ 7.39-7.24 (m, 5H), 7.17 (s, 1H), 7.12 (s, 1H), 4.14 (m, 1H), 4.00 (s, 3H), 3.97 (s, 3H), 3.59 (s, 2H), 2.91 (br, d, *J* = 11.5 Hz, 2H), 2.37 (br, t, *J* = 11.5 Hz, 2H), 2.22 (dd, J_1 = 11.5, 3.6 Hz, 2H), 1.85 (qd, *J* = 11.5 Hz, 3.6 Hz, 2H). MS (ESI) *m/z* 430.1 $[M+H]^+$. HRMS (ESI) *m/z* $[M+H]^+$ calcd for $C_{22}H_{24}ClN_3O_2S$: 430.1356, found: 430.1345.

Supplementary Material

Refer to Web version on PubMed Central for supplementary material.

Acknowledgments

S. Sundriyal acknowledges European Commission for awarding Marie Curie International Incoming Fellowship (Agreement No. 299857). This work was supported by Bill and Melinda Gates Foundation Grand Challenge Exploration Award OPP1008567 and a European Research Council PLASMOESCAPE grant (A.S.). N.A.M. was supported in part by a Pasteur Foundation of New York fellowship. N.S. was supported by a Royal Thai Government Scholarship and the EPSRC-funded Institute of Chemical Biology Doctoral Training Centre. This work was also supported by funding from the U.S. National Institutes of Health (J.J., R01GM103893). We thank Miss Jennifer Auer for additional help with the parasite culture experiments.

References and Notes

1. [January 2014] http://www.who.int/malaria/media/world_malaria_report_2013/en/index.html
2. a D'Alessandro U, Buttiens H. Trop. Med. Int. Health. 2001; 6:845–848. [PubMed: 11703837] b Petersen I, Eastman R, Lanzer M. FEBS Lett. 2011; 585:1551–1562. [PubMed: 21530510]
3. Gogtay N, Kannan S, Thatte UM, Olliaro PL, Sinclair D. Cochrane Database Syst. Rev. 2013; 10:Cd008492. [PubMed: 24163021]
4. a Noedl H, Socheat D, Satimai W. New Engl. J. Med. 2009; 361:540–541. [PubMed: 19641219] b Dondorp AM, Nosten F, Yi P, Das D, Phyo AP, Tarning J, Lwin KM, Ariey F, Hanpithakpong W, Lee SJ, Ringwald P, Silamut K, Imwong M, Chotivanich K, Lim P, Herdman T, An SS, Yeung S,

Singhasivanon P, Day NP, Lindegardh N, Socheat D, White NJ. New Engl. J. Med. 2009; 361:455–467. [PubMed: 19641202]

5. Callebaut I, Prat K, Meurice E, Mornon JP, Tomavo S. BMC Genomics. 2005; 6:100–120. [PubMed: 16042788]
6. a Balaji S, Babu MM, Iyer LM, Aravind L. Nucleic Acids Res. 2005; 33:3994–4006. [PubMed: 16040597] b De Silva EK, Gehrke AR, Olszewski K, Leon I, Chahal JS, Bulyk ML, Llinas M. Proc. Natl. Acad. Sci. USA. 2008; 105:8393–8398. [PubMed: 18541913]
7. a Coleman BI, Duraisingh MT. Cell. Microbiol. 2008; 10:1935–1946. [PubMed: 18637022] b Duffy MF, Selvarajah SA, Josling GA, Petter M. Brief. Funct. Genomics. 2013
8. Ponts N, Fu L, Harris Elena Y. Zhang J, Chung D.-Won D. Cervantes Michael C. Prudhomme J, Atanasova-Penichon V, Zehraoui E, Bunnik Evelien M. Rodrigues Elisandra M. Lonardi S, Hicks Glenn R. Wang Y, Le Roch Karine G. Cell Host Microbe. 2013; 14:696–706. [PubMed: 24331467]
9. a Miao J, Fan Q, Cui L, Li J, Li J, Cui L. Gene. 2006; 369:53–65. [PubMed: 16410041] b Trelle MB, Salcedo-Amaya AM, Cohen AM, Stunnenberg HG, Jensen ON. J. Proteome Res. 2009; 8:3439–3450. [PubMed: 19351122]
10. a Freitas-Junior LH, Hernandez-Rivas R, Ralph SA, Montiel-Condado D, Ruvalcaba-Salazar OK, Rojas-Meza AP, Mancio-Silva L, Leal-Silvestre RJ, Gontijo AM, Shorte S, Scherf A. Cell. 2005; 121:25–36. [PubMed: 15820676] b Jiang L, Lopez-Barragan MJ, Jiang H, Mu J, Gaur D, Zhao K, Felsenfeld G, Miller LH. Proc. Natl. Acad. Sci. USA. 2010; 107:2224–2229. [PubMed: 20080673] c Baruch DI, Pasloske BL, Singh HB, Bi X, Ma XC, Feldman M, Taraschi TF, Howard RJ. Cell. 1995; 82:77–87. [PubMed: 7541722] d Su XZ, Heatwole VM, Wertheimer SP, Guinet F, Herrfeldt JA, Peterson DS, Ravetch JA, Wellems TE. Cell. 1995; 82:89–100. [PubMed: 7606788] e Smith JD, Chitnis CE, Craig AG, Roberts DJ, Hudson-Taylor DE, Peterson DS, Pinches R, Newbold CI, Miller LH. Cell. 1995; 82:101–110. [PubMed: 7606775]
11. a Cui L, Miao J, Cui L. Antimicrob. Agents Chemother. 2007; 51:488–494. [PubMed: 17145789] b Cui L, Miao J, Furuya T, Fan Q, Li X, Rathod PK, Su XZ, Cui L. Eukaryot. Cell. 2008; 7:1200–1210. [PubMed: 18487348]
12. a Andrews KT, Tran TN, Lucke AJ, Kahnberg P, Le GT, Boyle GM, Gardiner DL, Skinner-Adams TS, Fairlie DP. Antimicrob. Agents Chemother. 2008; 52:1454–1461. [PubMed: 18212103] b Darkin-Rattray SJ, Gurnett AM, Myers RW, Dulski PM, Crumley TM, Allocco JJ, Cannova C, Meinke PT, Colletti SL, Bednarek MA, Singh SB, Goetz MA, Dombrowski AW, Polishook JD, Schmatz DM. Proc. Natl. Acad. Sci. USA. 1996; 93:13143–13147. [PubMed: 8917558] c Dow GS, Chen Y, Andrews KT, Caridha D, Gerena L, Gettayacamin M, Johnson J, Li Q, Melendez V, Obaldia N 3rd, Tran TN, Kozikowski AP. Antimicrob. Agents Chemother. 2008; 52:3467–3477. [PubMed: 18644969] d Prusty D, Mehra P, Srivastava S, Shivange AV, Gupta A, Roy N, Dhar SK. FEMS Microbiol. Lett. 2008; 282:266–272. [PubMed: 18397290]
13. Malmquist NA, Moss TA, Mecheri S, Scherf A, Fuchter MJ. Proc. Natl. Acad. Sci. USA. 2012; 109:16708–16713. [PubMed: 23011794]
14. Kubicek S, O'Sullivan RJ, August EM, Hickey ER, Zhang Q, Teodoro ML, Rea S, Mechtler K, Kowalski JA, Homon CA, Kelly TA, Jenuwein T. Mol. Cell. 2007; 25:473–481. [PubMed: 17289593]
15. a Liu F, Chen X, Allali-Hassani A, Quinn AM, Wasney GA, Dong A, Barsyte D, Kozieradzki I, Senisterra G, Chau I, Siarheyeva A, Kireev DB, Jadhav A, Herold JM, Frye SV, Arrowsmith CH, Brown PJ, Simeonov A, Vedadi M, Jin J. J. Med. Chem. 2009; 52:7950–7953. [PubMed: 19891491] b Liu F, Chen X, Allali-Hassani A, Quinn AM, Wigle TJ, Wasney GA, Dong A, Senisterra G, Chau I, Siarheyeva A, Norris JL, Kireev DB, Jadhav A, Herold JM, Janzen WP, Arrowsmith CH, Frye SV, Brown PJ, Simeonov A, Vedadi M, Jin J. J. Med. Chem. 2010; 53:5844–5857. [PubMed: 20614940] c Liu F, Barsyte-Lovejoy D, Allali-Hassani A, He Y, Herold JM, Chen X, Yates CM, Frye SV, Brown PJ, Huang J, Vedadi M, Arrowsmith CH, Jin J. J. Med. Chem. 2011; 54:6139–6150. [PubMed: 21780790] d Chang Y, Ganesh T, Horton JR, Spannhoff A, Liu J, Sun A, Zhang X, Bedford MT, Shinkai Y, Snyder JP, Cheng X. J. Mol. Biol. 2010; 400:1–7. [PubMed: 20434463] e Vedadi M, Barsyte-Lovejoy D, Liu F, Rival-Gervier S, Allali-Hassani A, Labrie V, Wigle TJ, Dimaggio PA, Wasney GA, Siarheyeva A, Dong A, Tempel W, Wang SC, Chen X, Chau I, Mangano TJ, Huang XP, Simpson CD, Pattenden SG, Norris JL,

Kireev DB, Tripathy A, Edwards A, Roth BL, Janzen WP, Garcia BA, Petronis A, Ellis J, Brown PJ, Frye SV, Arrowsmith CH, Jin J. Nat. Chem. Biol. 2011; 7:566–574. [PubMed: 21743462]

16. Dembele L, Franetich JF, Lorthiois A, Gego A, Zeeman AM, Kocken CH, Le Grand R, Dereuddre-Bosquet N, van Gemert GJ, Sauerwein R, Vaillant JC, Hannoun L, Fuchter MJ, Diagana TT, Malmquist NA, Scherf A, Snounou G, Mazier D. Nat. Med. 2014; 20:307–312. [PubMed: 24509527]
17. Chang Y, Zhang X, Horton JR, Upadhyay AK, Spannhoff A, Liu J, Snyder JP, Bedford MT, Cheng X. Nat. Struct. Mol. Biol. 2009; 16:312–317. [PubMed: 19219047]
18. Wu H, Min J, Lunin VV, Antoshenko T, Dombrovski L, Zeng H, Allali-Hassani A, Campagna-Slater V, Vedadi M, Arrowsmith CH, Plotnikov AN, Schapira M. PloS one. 2010; 5:e8570. [PubMed: 20084102]
19. Alignment was performed in Uniprot using complete sequences of human G9a (Q96KQ97, EHMT92_HUMAN) and putative histone methyltransferase of P. falciparum (C96KTD92, SET91_PLAF97, evidence at transcript level).
20. Nguyen KT, Li F, Poda G, Smil D, Vedadi M, Schapira M. J. Chem. Inf. Model. 2013; 53:681–691. [PubMed: 23410263]
21. Malmquist N, et al. J. Antimicrob. Chemother. (Submitted).
22. Liu F, Barsyte-Lovejoy D, Li F, Xiong Y, Korboukh V, Huang X-P, Allali-Hassani A, Janzen WP, Roth BL, Frye SV, Arrowsmith CH, Brown PJ, Vedadi M, Jin J. J. Med. Chem. 2013; 56:8931–8942. [PubMed: 24102134]
23. Smilkstein M, Sriwilaijaroen N, Kelly JX, Wilairat P, Riscoe M. Antimicrob. Agents Chemother. 2004; 48:1803–1806.
24. [December, 2013] http://www.rdkit.org/
25. Coteron JM, Marco M. a. Esquivias J, Deng X, White KL, White J, Koltun M, El Mazouni F, Kokkonda S, Katneni K, Bhamidipati R, Shackleford DM, Angulo-Barturen I. i. Ferrer SB, Jimenez-Diaz M. a. B. n. Gamo F-J, Goldsmith EJ, Charman WN, Bathurst I, Floyd D, Matthews D, Burrows JN, Rathod PK, Charman SA, Phillips MA. J. Med. Chem. 2011; 54:5540–5561. [PubMed: 21696174]
26. Obach RS. Drug. Metab. Dispos. 1999; 27:1350–1359. [PubMed: 10534321]
27. Ring BJ, Chien JY, Adkison KK, Jones HM, Rowland M, Jones RD, Yates JW, Ku MS, Gibson CR, He H, Vuppugalla R, Marathe P, Fischer V, Dutta S, Sinha VK, Bjornsson T, Lave T, Poulin P. J. Pharm. Sci. 2011; 100:4090–4110.

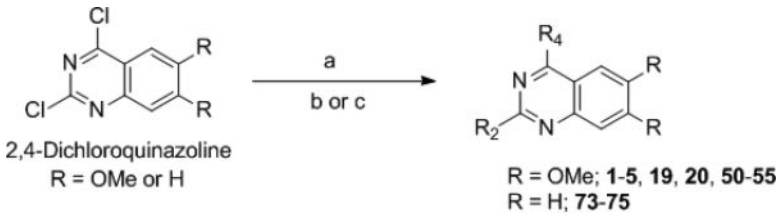

Scheme 1.

Synthesis of 2,4-disubstituted quinazolines Reactions and Conditions: (a) different amines, Et_3N (or DIEA), THF (or DMF), r.t., 18 h; (b) different amines (10 eqv), microwave, toluene (or neat), 130-185 °C, 30-50 min (c) *i*-PrOH, 4 M HCl/dioxane, microwave, 160 °C, 15 min.

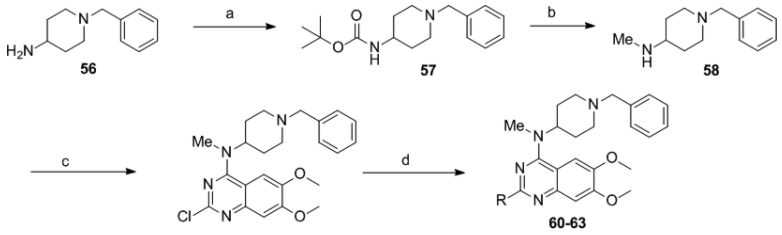

Scheme 2.

Synthesis of quinazolines analogues with a *N*-Me group at position-4. Reactions and Conditions: (a) Boc_2O, Et_3N, DCM, 17 h, r.t.; (b) $LiAlH_4$, THF, 3 days; (c) 2,4-dichloro-6,7-dimethoxyquinazoline, Et_3N, THF, 18 h, r.t.; (d) different amines (10 eqv), toluene, reflux, 18 h.

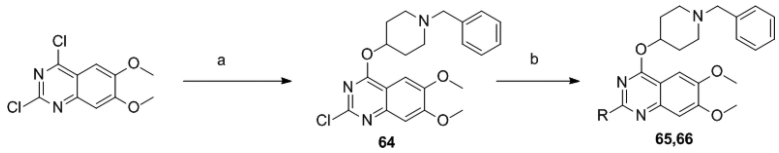

Scheme 3.

Synthesis of quinazolines analogues with an oxygen atom at position-4. Reactions and Conditions: (a) K*O*-*t*Bu, DMSO, 1-Benzyl-4-piperidinol, 2 h, r.t.; (b) cyclic amines (10 eqv), toluene, reflux, 18 h.

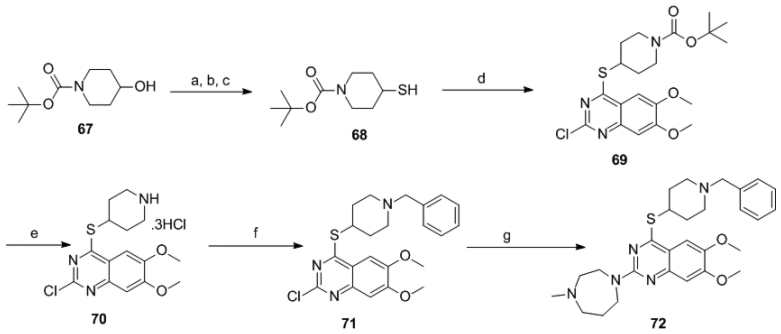

Scheme 4.

Synthesis of quinazolines analogues with a sulphur atom at position-4. Reactions and Conditions: (a) MsCl, Et_3N, DCM, 0 °C, 1 h; (b) KSAc, DMF, 60 °C, 16 h; (c) $NaBH_4$, MeOH, r.t., 20 min; (d) NaH, THF, 0 °C, 20 min, then, 2,4-dichloro-6,7-dimethoxyquinazoline; (e) 4*N* HCl in dioxane, r.t. 16 h; (f) benzaldehyde, $Na(AcO)_3BH$, Et_3N, AcOH, EtOH, r.t., 16 h; (g) *N*-methyl homopiperazine (10 eqv), toluene, reflux, 18 h.

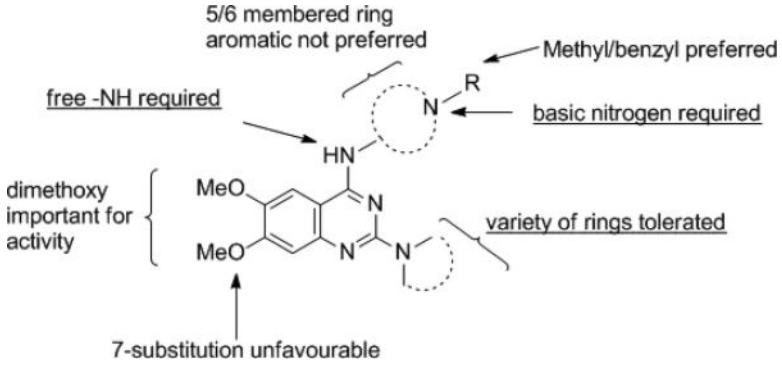

Figure 1.

SAR of quinazoline scaffold for *Pf3D7* activity. The underlined features are conserved for human G9a/GLP inhibition.

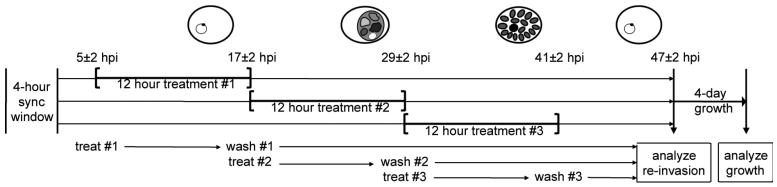

A

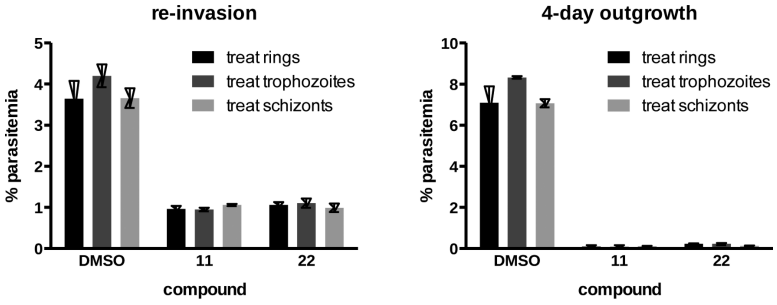

B

C

Figure 2.

Stage-dependent antimalarial activity. (A) Synchronized *P. falciparum* parasites were treated with DMSO or 10x IC_{50} values of compounds **11** or **22** for three distinct 12 hour periods of the intraerythrocytic life cycle. (B) Re-invasion of treated parasites at 47 hours post-invasion was quantified by flow cytometry. (C) After 12-hour treatment, parasites were washed, diluted, and allowed to grow for four days after which parasitemia was measured by flow cytometry. Data are mean ± SD of 30,000 RBCs from duplicate samples.

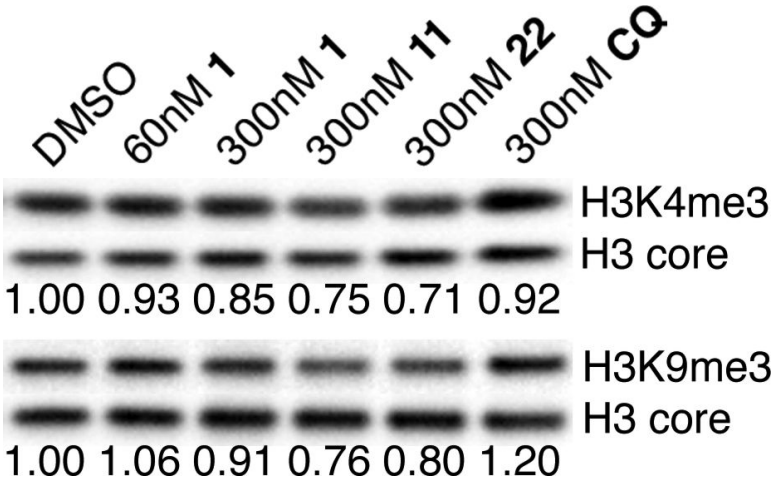

Figure 3.

Histone methylation levels in treated parasites. *P. falciparum* 3D7 parasites were treated with the indicated compounds or DMSO vehicle control for 12 hours. Specific histone H3K4me3 and H3K9me3 levels were quantified by densitometry, normalized to histone H3 core signal, and resulting methylation levels relative to DMSO control treated parasites are indicated below each pair of methylation specific and corresponding core histone H3 bands

Table 1

SAR for R_2 and R_4 substituents

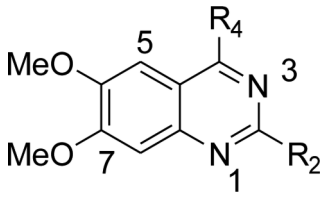

Cmpd ID	R4	R2	Pf3D7 IC_{50} (nM)	HepG2 IC_{50} (μM)	HepG2/Pf3D7	clogP	PSA
1 BIX01294	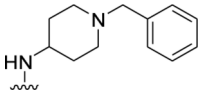	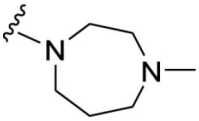	43.4	4.8	110.6	3.86	65.99
2	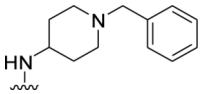	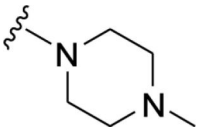	18.5	5.5	297.3	3.48	65.99
3	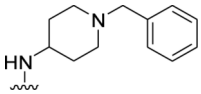	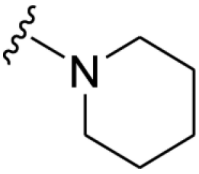	23.3	4.7	201.8	4.71	62.75
4	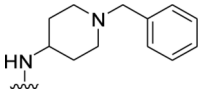	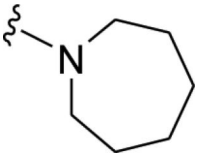	29.1	3.8	130.6	5.10	62.75
5	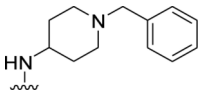	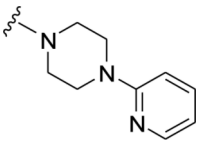	26.5	2.6	98.2	4.44	78.88
6	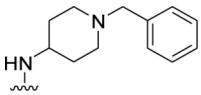	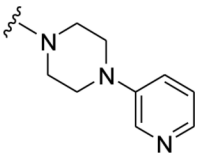	67.6	4.9	72.5	4.44	78.88
7	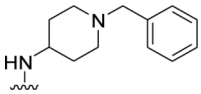	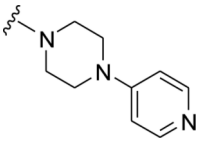	54.0	4.9	90.8	4.44	78.88

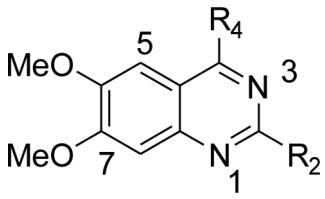

Cmpd ID	R4	R2	Pf3D7 IC_{50} (nM)	HepG2 IC_{50} (μM)	HepG2/Pf3D7	clogP	PSA
8	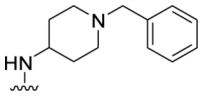	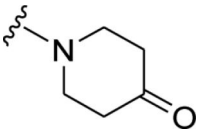	30.3	10.7	353.2	3.89	79.82
9	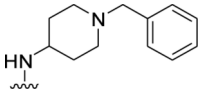	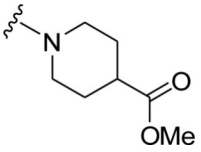	41.7	9.6	230.3	4.11	89.05
10	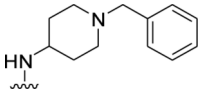	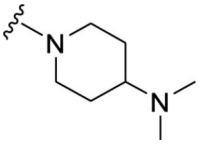	36.6	5.9	161.3	4.25	65.99
11	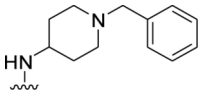	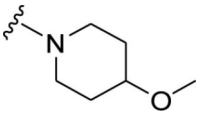	37.6	10.1	268.7	4.34	71.98
12	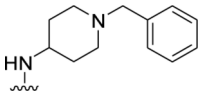	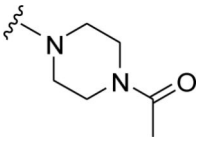	47.0	11.2	238.3	4.53	79.82
13	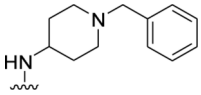	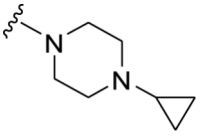	45.4	7.9	174.1	5.35	62.75
14	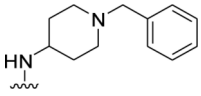	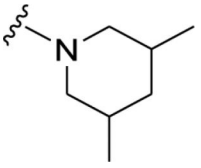	67.4	3.6	53.5	5.21	62.75
15	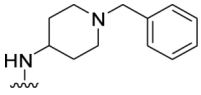	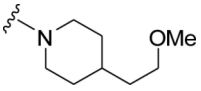	80.4	6.3	78.4	4.98	71.98

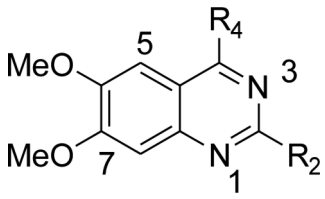

Cmpd ID	R4	R2	Pf3D7 IC_{50} (nM)	HepG2 IC_{50} (μM)	HepG2/Pf3D7	clogP	PSA
16	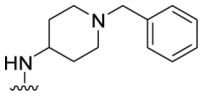	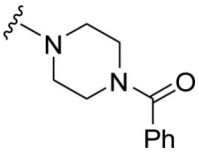	60.6	6.4	105.7	5.82	79.82
17	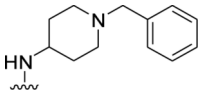	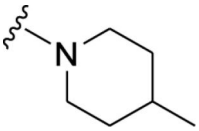	76.0	5.4	71.1	4.96	62.75
18	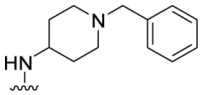	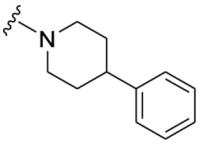	71.5	6.1	85.4	6.11	62.75
19	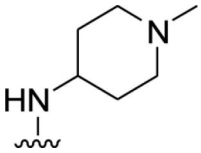	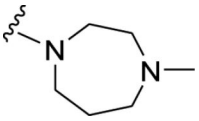	>300	ND	-	2.30	65.99
20	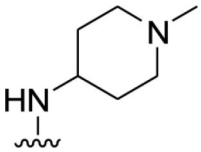	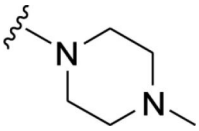	>300	ND	-	1.90	65.99
21	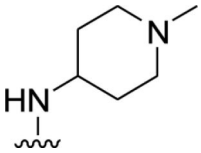	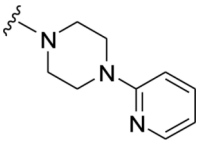	56.5	5.5	97.4	2.88	78.88
22	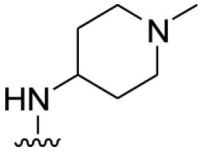	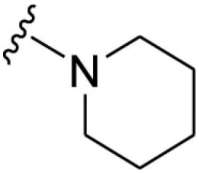	36.6	14.2	388	3.14	62.75

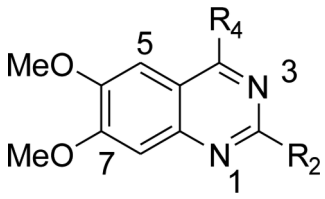

Cmpd ID	R4	R2	Pf3D7 IC_{50} (nM)	HepG2 IC_{50} (μM)	HepG2/Pf3D7	clogP	PSA
23	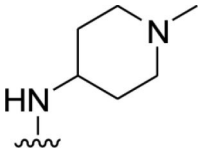	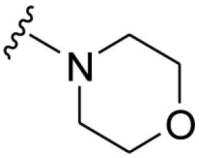	173.8	26.8	154.3	1.99	71.98
24	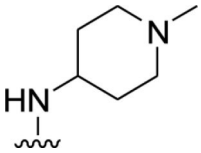	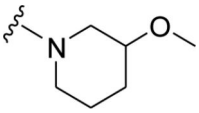	53.4	10.8	202.3	2.77	71.98
25	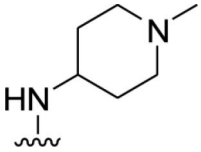	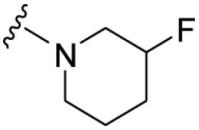	19.6	11.7	597	3.09	62.75
26	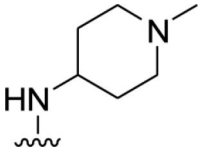	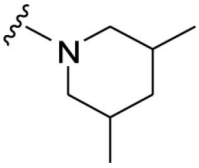	18.7	5.7	304.9	3.64	62.75
27	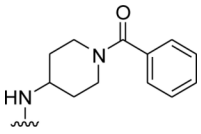	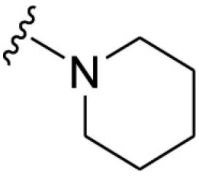	369.0	ND	-	4.35	79.82
28	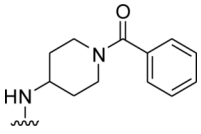	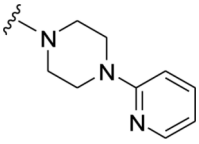	246.6	ND	-	4.08	95.95
29	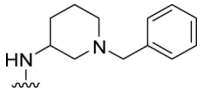	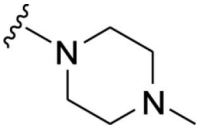	197.3	10.5	53.3	3.48	65.99

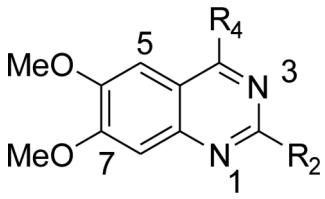

Cmpd ID	R4	R2	Pf3D7 IC_{50} (nM)	HepG2 IC_{50} (μM)	HepG2/Pf3D7	clogP	PSA
30	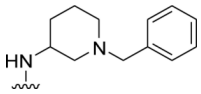	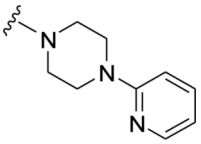	144.5	6.5	45	4.44	78.88
31	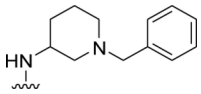	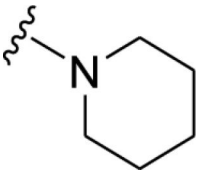	178.5	6.3	35.3	4.71	62.75
32	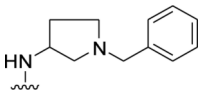	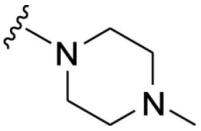	330.4	ND	-	3.09	65.99
33	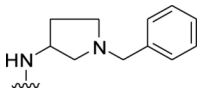	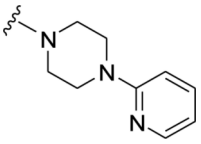	92.9	5.6	60.3	4.06	78.88
34	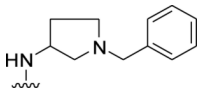	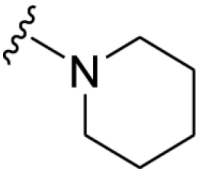	94.3	6.3	66.9	4.32	62.75
35	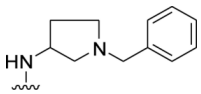	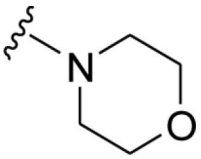	152.4	15.3	100.4	3.17	71.98
36	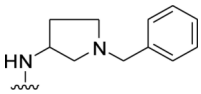	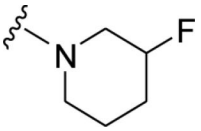	110.6	6.5	58.8	4.27	62.75

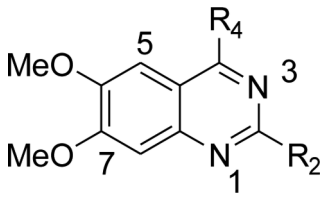

Cmpd ID	R4	R2	Pf3D7 IC_{50} (nM)	HepG2 IC_{50} (μM)	HepG2/Pf3D7	clogP	PSA
37	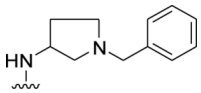	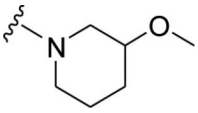	111.0	10.8	97.3	3.95	71.98
38	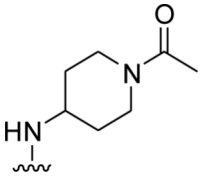	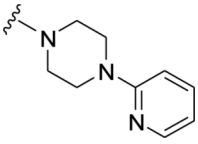	335.0	ND	-	2.79	95.95
39	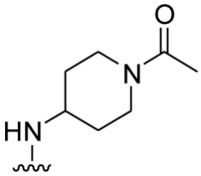	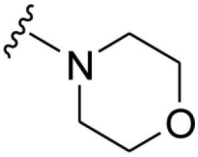	>2000	ND	-	1.91	89.05
40	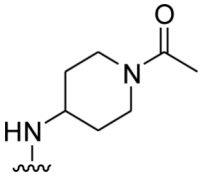	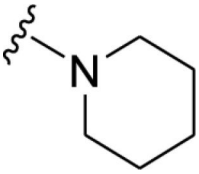	685.5	ND	-	3.06	79.82
41	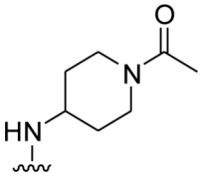	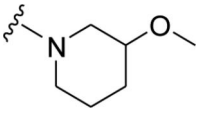	>2000	ND	-	2.68	89.05
42	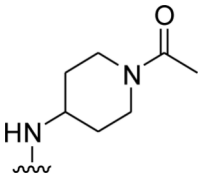	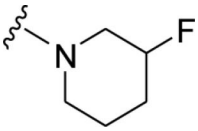	>2000	ND	-	3.01	79.82

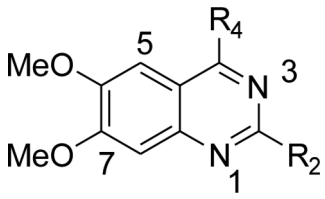

Cmpd ID	R4	R2	Pf3D7 IC_{50} (nM)	HepG2 IC_{50} (μM)	HepG2/Pf3D7	clogP	PSA
43	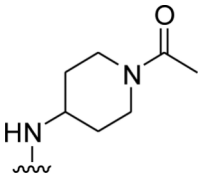	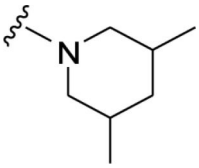	107.4	17.8	165.8	3.55	79.82
44	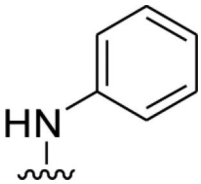	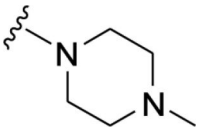	569.6	ND	-	3.142	62.75
45	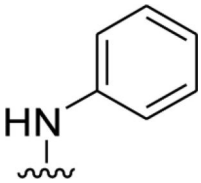	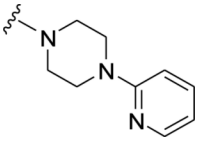	194.5	28.3	145.6	4.11	75.64
46	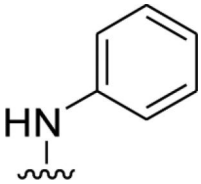	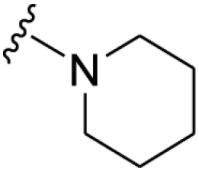	161.4	ND	-	4.38	59.51
47	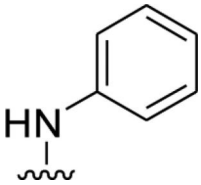	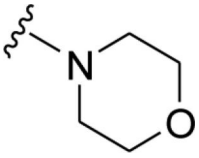	922.6	ND	-	3.23	68.74
48	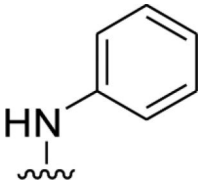	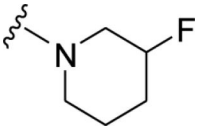	272.3	ND	-	4.33	59.51

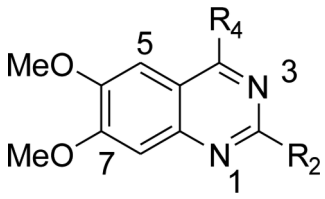

Cmpd ID	R4	R2	Pf3D7 IC_{50} (nM)	HepG2 IC_{50} (μM)	HepG2/Pf3D7	clogP	PSA
49	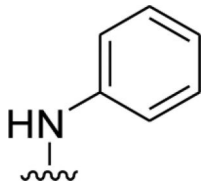	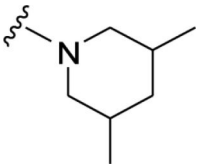	76.6	12.2	159.3	4.87	59.51
50	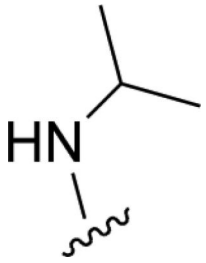	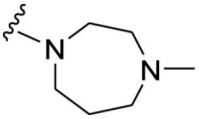	322.5	ND	-	2.61	62.75
51	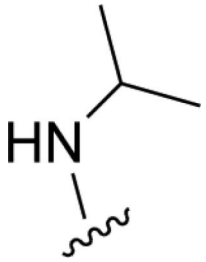	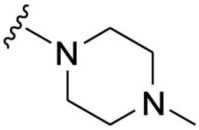	>300	ND	-	2.22	62.75
52	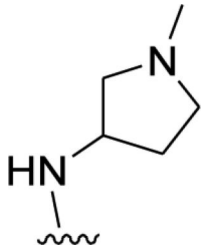	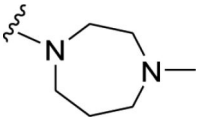	>300	ND	-	1.90	65.99
53	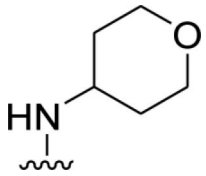	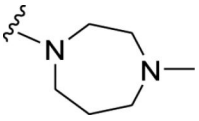	>300	ND	-	2.38	71.98

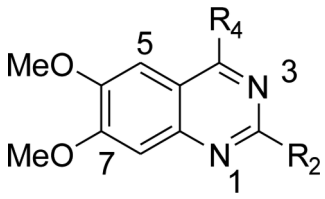

Cmpd ID	R4	R2	Pf3D7 IC_{50} (nM)	HepG2 IC_{50} (μM)	HepG2/Pf3D7	clogP	PSA
54	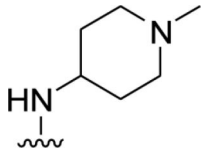	-$N(Et)_2$	27.6	>10	-	3.00	62.75
55	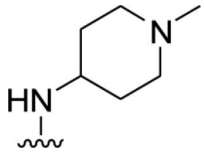	-$N(Me)_2$	34.4	>10	-	2.22	62.75

Table 2

SAR of 4-amino region

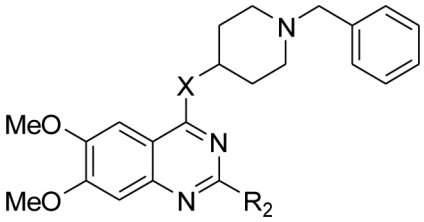

Cmpd ID	X	R2	*Pf3*D7 IC_{50} (nM)	HepG2 IC_{50} (μM)	HepG2/Pf3D7	ClogP	PSA
1 BIX01294	NH	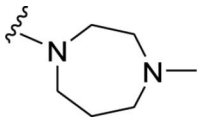	43.4	4.8	110.6	3.86	65.99
60	N-Me	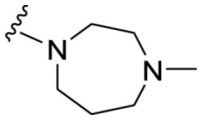	158.7	6.0	37.9	3.89	57.2
3	NH	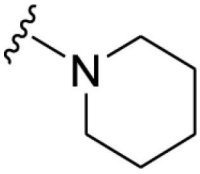	23.3	4.7	201.8	4.71	62.75
61	N-Me	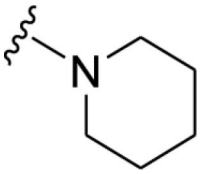	495.1	8.1	16.4	4.74	53.96
4	NH	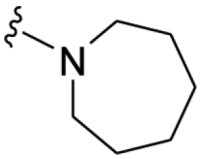	29.1	3.8	130.6	5.10	62.75
62	N-Me	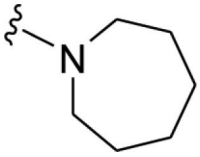	399.5	5.4	13.6	5.13	53.96

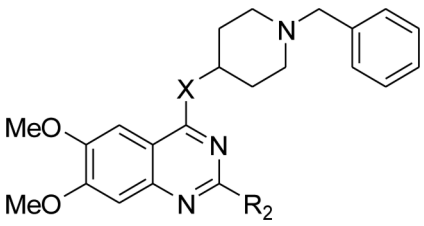

Cmpd ID	X	R2	*Pf3*D7 IC_{50} (nM)	HepG2 IC_{50} (μM)	HepG2/Pf3D7	ClogP	PSA
5	NH	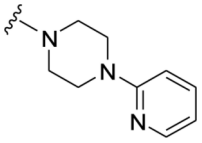	26.5	2.6	98.2	4.44	78.88
63	N-Me	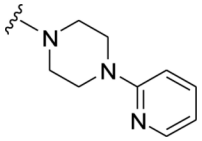	472.3	9.6	20.4	4.47	70.09
65	O	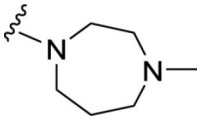	1464	7.9	5.4	3.83	63.19
66	O	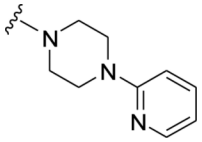	2061	15.7	7.7	4.41	76.08
72	S	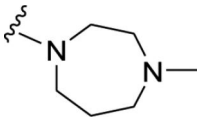	1541	10.2	6.7	4.55	53.96

Table 3

SAR of 6,7-dimetoxy region

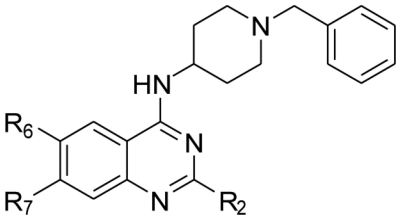

Cmpd ID	R_2	$R_6 = R_7$	*Pf3*D7 IC_{50} (nM)	HepG2 IC_{50} (μM)	HepG2/Pf3D7	clogP	TPSA
1 BIX01294	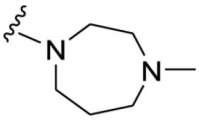	-OMe	43.4	4.8	110.6	3.86	65.99
73	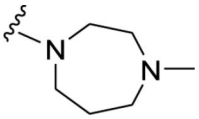	H	100.7	7.0	69.6	3.85	47.53
3	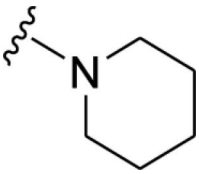	-OMe	23.3	4.7	201.8	4.71	62.75
74	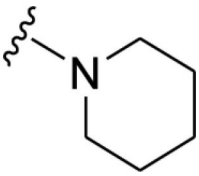	H	384.6	4.0	10.5	4.70	44.29
5	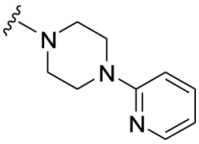	-OMe	26.5	2.6	98.2	4.44	78.88
75	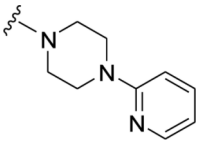	H	353.6	5.0	14.2	4.43	60.42

Table 4

SAR of position-7 substituent

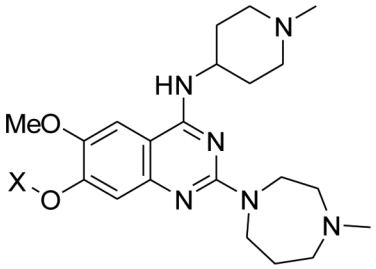

Cmpd ID	X	*Pf3*D7 IC_{50} (nM)	HepG2 IC_{50} (μM)	HepG2/Pf3D7	ClogP	TPSA
76 (TM2-115)	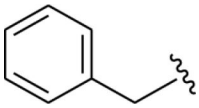	42.7	4.7	110.1	3.86	65.99
77	-OH	>2000	ND	-	1.99	76.99
78	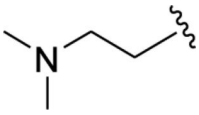	>2000	ND	-	2.23	69.23
79	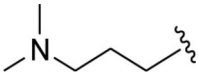	>2000	ND	-	2.62	69.23
80	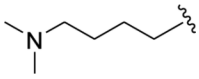	>2000	ND	-	3.01	69.23
81	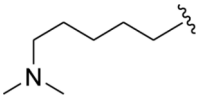	>2000	ND	-	3.40	69.23
82	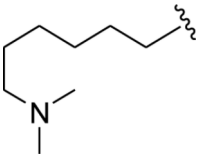	>2000	ND	-	3.79	69.23
83	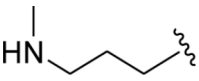	>2000	ND	-	2.28	78.02
84	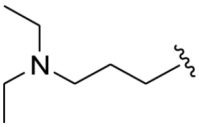	>2000	ND	-	3.40	69.23

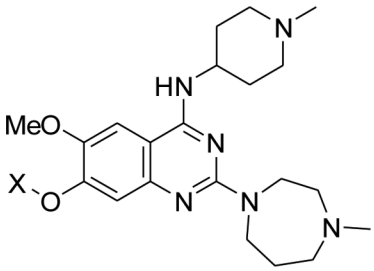

Cmpd ID	X	*Pf*3D7 IC_{50} (nM)	HepG2 IC_{50} (μM)	HepG2/Pf3D7	ClogP	TPSA
85	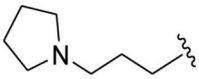	>2000	ND	-	3.15	69.23
86	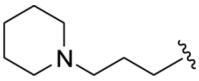	>2000	ND	-	3.54	69.2
87	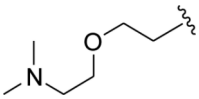	>2000	ND	-	2.24	78.46
88	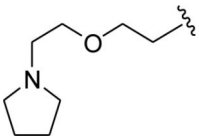	>2000	ND	-	2.78	78.46
89	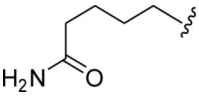	>2000	ND	-	2.32	109.1
90	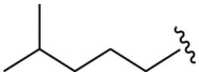	150	3.0	9.4	4.10	65.99
91	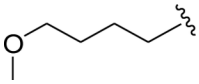	319.1	ND	-	3.09	75.22

Table 5

Pharmacokinetics and physicochemical properties of a few representative compounds

	1	**76**	**11**	**22**
		BIX-01294[b]	**TM2-115**[b]	
*Pf*3D7 IC_{50} (nM)	43.4	42.7	37.6	36.6
HepG2 IC_{50} (nM)	4800	4700	10100	14200
HepG2/3D7	110.6	110.1	268.6	388.0
rat plasma $t_{1/2}$ (h)	>4h	>4h	>4h	>4h
MW	491	491	492	386
clogP	3.86	3.86	4.34	3.14
logD pH 3	0.5	0.9	1.4	1
logD pH 7.4	5	4.2	4.2	3.8
solubility pH 2 (μg/ml)	>100	>100	>100	50-100
solubility pH 6.5 (μg/ml)	>100	50-100	50-100	6.3-12.5
rat microsome $t_{1/2}$ (min)	53	28	184	97
in vitro CL_{int} (μl/min/mg protein)	33	62	9	18
Predicted E_H[a]	0.45	0.61	0.19	0.31

[a] predicted *in vivo* hepatic extraction ratio

[b] data for **1** and **76** taken from reference 21